Photodetachment of the negative iodine ion including relaxation effects

Vojislav Radojević
Marmara University, Istanbul, Turkey

Hugh P. Kelly
Department of Physics, University of Virginia, Charlottesville, Virginia 22901
(Received 21 November 1991)

The effects of relaxation on the photodetachment of the iodine negative ion are calculated using the recently developed relativistic random-phase approximation with relaxation. In this method the outgoing electron is calculated in the field of the relaxed negative ion with one electron removed (i.e., in the field of the atom). Overlap integrals between orbitals of the initial and final states are included. It is found that the relaxation effects for the negative iodine atom are significantly larger than those for the corresponding neutral atom Xe. Comparison is made with results calculated by the relativistic random-phase approximation and with experiment near the $5p$ threshold.

PACS number(s): 32.80.Fb

It is well known that relaxation effects should be included in photoionization calculations [1–4] to bring cross sections of the Ba ($Z=56$) $4d$ subshell into agreement with experiment. A theoretical study of the barium $4d$ shell was recently performed [4] using the relativistic random-phase approximation (RRPA) [5], modified to include relaxation effects (RRPAR), to understand new experimental data and previous theoretical results (see Ref. [4] for relevant references). The RRPAR was also used in a calculation of the photoionization of the $4d$ and $3d$ shells of xenon ($Z=54$) [6], improving agreement with observations compared to calculations without relaxation.

The subject of the present study is the investigation of relaxation effects in the photodetachment of the iodine ($Z=53$) negative ion in order to see whether inclusion of relaxation introduces such changes in the photodetachment parameters, as has been the case in the previous studies of barium [4] and xenon [6]. The photodetachment of the outer shells of the negative halogen ions (F^-, Cl^-, Br^- and I^-) was recently studied [7] using the RRPA [5], and reasonable agreement with the limited experimental data available was obtained. In the present work we have extended the previous RRPA calculations [7] of the photodetachment of I^- to the $4d$ shell and also have included relaxation effects in calculations of the $5s$, $5p$, and $4d$ shells.

In the present work, channels obtained by dipole excitation of the appropriate subshells considered are included in our calculations. There are 13 such jj-coupled channels:

$$5p_{3/2} \rightarrow d_{5/2'} d_{3/2'} s_{1/2} ,$$

$$5p_{1/2} \rightarrow d_{3/2'} s_{1/2}, \quad 5s_{1/2} \rightarrow p_{3/2'} p_{1/2},$$

$$4d_{3/2} \rightarrow f_{5/2'} p_{3/2'} p_{1/2}, \quad 4d_{5/2} \rightarrow f_{7/2'} f_{5/2'} p_{3/2} .$$

Calculations were performed using the RRPA [5] method modified to include relaxation effects (RRPAR) [4]. The relaxation effects were included by performing the RRPA-type calculations and computing the excited-state orbitals in the V^{N-1} potential of the relaxed neutral iodine atom [4]. Overlaps between orbitals of the relaxed atom and the negative-ion ground state multiply the dipole matrix elements in these calculations and lead to reduction of the cross section of approximately 6% for the $5p$ subshell, 7% for the $5s$ subshell, and 17% for the $4d$ subshell. It is interesting to compare the presently calculated reduction of the $4d$ cross section of the iodine negative ion (17%) with the reduction of the $4d$ cross sections for xenon (11%) [6] and barium (20%) [4]. The photodetachment parameters for the $4d$ shell are also calculated in the strict (unrelaxed) RRPA.

We used for thresholds in the present RRPAR calculations either experimental values [8,9] available only for the outermost $5p$ subshells or ΔE_{SCF} (SCF being self-consistent-field results) values, which are defined as the differences between the total relativistic energies calculated self-consistently for the relaxed negative ion with a hole in the considered subshell (i.e., for the neutral atom) and the ground state of the negative ion. In the usual RRPA, ionization thresholds are given by absolute value of the Dirac-Hartree-Fock (DHF) eigenvalues. Table I contains calculated RRPA values (absolute values of DHF eigenvalues) and ΔE_{SCF} values, as well as available experimental threshold energies.

The results of our RRPAR calculations for the photodetachment cross section of the $5p$ and $5s$ shells are shown in Fig. 1 from the threshold to 90 eV photon energy, and are compared there with our previous RRPA calculations [7]. Since experimental data for photodetachment cross sections exist only for photon energies close to the threshold, we also show our calculated RRPAR results and the RRPA results [7] from the threshold up to 7 eV in the inset of Fig. 1, and compare them there with experimental data [10,11]. However, the experimental data do not decisively favor one or another result in this region. As seen from Fig. 1, the present RRPAR theoreti-

TABLE I. Photoionization thresholds for subshells of the iodine negative ion (I^-) included in present work. Presented are calculated DHF (used in RRPA) and ΔE_{SCF} values, and available experimental (expt.) data.

	DHF (RRPA)[a]		ΔE_{SCF}[b]		Expt.	
Subshell	(a.u.)	(eV)	(a.u.)	(eV)	(a.u.)	(eV)
$5p_{3/2}$	0.113 53	3.0893	0.080 27	2.1824	0.112 42	3.0951[c]
$5p_{1/2}$	0.154 60	4.2086	0.115 52	3.1435	0.147 03	4.001[d]
$5s_{1/2}$	0.608 38	16.5550	0.558 69	15.203		
$4d_{3/2}$	1.980 71	53.8980	1.762 47	47.959		
$4d_{5/2}$	2.084 19	55.7342	1.826 57	49.704		

[a]Absolute value of single-particle eigenvalue from Dirac-Hartree-Fock (DHF) calculations, this work.
[b]Difference of self-consistent DHF calculated energies for the relaxed negative iodine ion with a hole in a given subshell and the ground state of the negative ion.
[c]Reference 8.
[d]The experimental value of the second $5p_{1/2}$ threshold is obtained by adding the observed value of the splitting of the ^2P term (Ref. [9]) to the value of the first threshold.

cal data are somewhat different from the previously calculated RRPA results [7], which do not account for relaxation effects. One can see that in the region of energies below and above the first maximum of the 5*p* cross section at about 11 eV the RRPAR cross section values are below the RRPA results while around the maximum near 83 eV the RRPAR velocity becomes larger than the RRPA cross section. Although both approaches give cross-section curves from the threshold up to the minimum at about 55 eV of essentially the same form, the difference between them cannot be ascribed to the reduction of the RRPA cross sections due to the overlap of relaxed and unrelaxed wave functions. For energies above the first maximum, the RRPAR velocity is first close to the RRPA cross section, then, at somewhat higher energies up to the second maximum of the 5*p* cross section (at about 83 eV) the RRPAR velocity and length come close to one another and become practically identical with RRPA results. The 5*s* cross section in the RRPAR and RRPA methods differ greatly from the 5*s* threshold to the minimum at about 33 eV, and practically coincide for

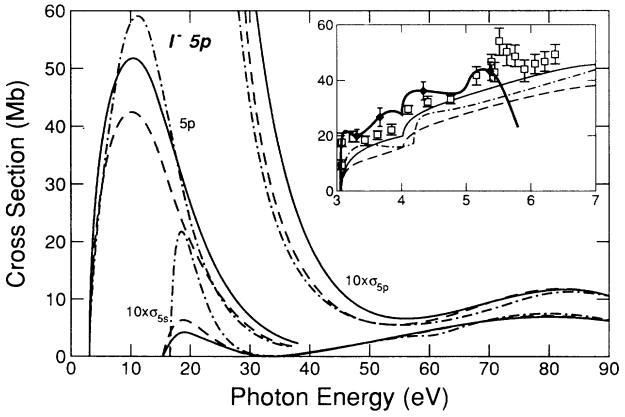

FIG. 1. Photodetachment cross section for the 5*p* and 5*s* shells of I^-. —— (solid line), RRPAR result in length form, — — — (dashed line), RRPAR results in velocity form; —·—·— (dash-dotted line), RRPA results (Ref. [7]) in length form. (Velocity form RRPA results from Ref. [7] are indistinguishable from the length form in the scale of figure almost everywhere except in the very vicinity of the peak, where they are smaller than length results by, at most, a few percent.) In the inset is shown the photodetachment cross section for photon energies close to the threshold, where comparison is made with the only available experimental data from Ref. [10] (□) and Ref. [11], heavy solid line with (♦).

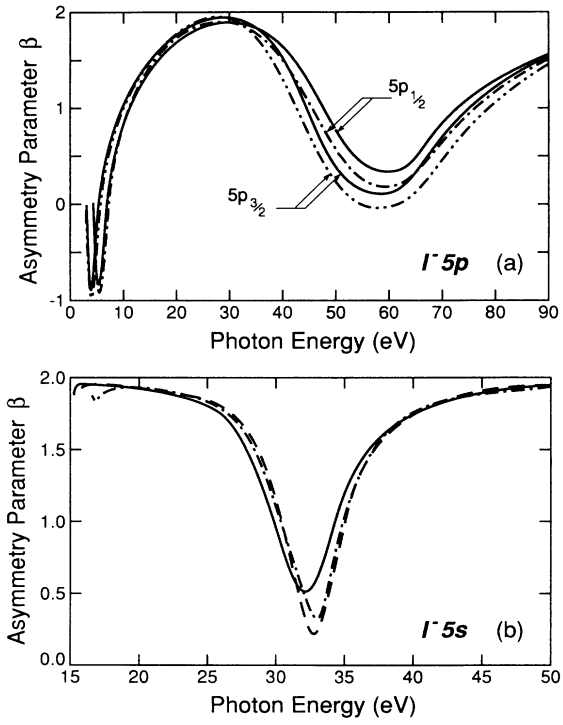

FIG. 2. Photoelectron angular asymmetry parameters β (a) for $5p_{3/2}$ and $5p_{1/2}$ subshells. ——, RRPAR results average of length and velocity forms. —·—·—·, RRPA results for $5p_{1/2}$. —··—, RRPA results for $5p_{3/2}$. (b) β for 5*s* subshell. ——, length form RRPAR result. — — —, velocity form RRPAR result ·—·—, RRPA results from Ref. [7].

higher energies.

The photoelectron angular distribution asymmetry parameters β for the $5p_{3/2}$ and $5p_{1/2}$ subshells are shown in Fig. 2(a), and for the $5s$ shell in Fig. 2(b). We have plotted our present results using the RRPAR method and also the RRPA results [7]. Although the present length and velocity RRPAR results for the $5p$ shell are not so close to one another as for the RRPA results, they are quite close, and we present only the average of length and velocity values in Fig. 2(a). The length and velocity forms of the RRPAR results mostly differ only in the region between 40 and 60 eV, but their difference does not exceed about 0.3 units of asymmetry parameter. One sees that relaxation effects are not very prominent for the β parameters of the $5p$ and $5s$ subshell of I .

Presently calculated photoionization parameters for the $4d$ shell are presented in Fig. 3. The results for the total $4d$ cross section in length and velocity form of the RRPAR, as well as in the RRPA method, are plotted in Fig. 3(a). Only one curve for the $4d$ cross section in the RRPA is presented in Fig. 3(a), since length and velocity forms practically coincide in the scale of the figure. One sees that, in the region of energies around the maximum of the $4d$ cross section, the difference of the RRPAR and the RRPA results cannot be completely accounted by reduction due to the overlap of relaxed and unrelaxed wave functions amounting to about 17%. For photon energies above 200 eV the difference of the two cross section results can be accounted by the overlap between the relaxed and unrelaxed wave functions with unrelaxed 17% larger than relaxed cross sections. However, this difference is not observable on the scale of Fig. 3(a), because of the relative smallness of the cross sections in this region. The photoelectron asymmetry parameters β for the $4d_{5/2}$ and $4d_{3/2}$ subshells are shown in Fig. 3(b) and exhibit some, but not striking, differences.

Usually various atomic properties of different atoms and ions change gradually with atomic number Z or number of electrons N, except for some atomic systems with the atomic number in the vicinity of $Z=54$ (xenon) such as Ba ($Z=56$). Such atomic systems contain the inner $4d$ shell, and significant changes occur in some cases involving excitations of the $4d$ subshell. Such behavior can be understood in terms of the well-known effective double-well structure of the potential for an f electron excited from the $4d$ shell [12], and small changes in potential may significantly alter the presence of the f electron in one or another potential well. In this work the relaxation effects are noticeably larger for the negative ion of iodine than for the xenon atom which is isoelectronic with it. This is not surprising since the electrons in the negative ion are less tightly bound than for the isoelectronic atom and removal of an electron should cause larger rearrangement effects.

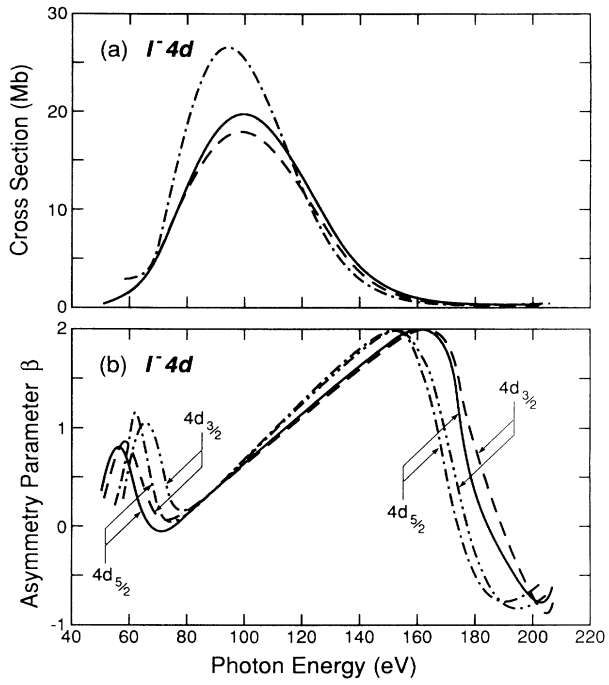

FIG. 3. The photodetachment parameters for the $4d$ subshell of I^-. (a) Total $4d$ cross section. —— (solid line), RRPAR results in length form; — — —, RRPAR results in velocity form; —·—·— (dash-dotted line). RRPA results. (b) angular asymmetry parameter β. ——, RRPAR results for the $4d_{5/2}$ subshell; — — — (dashed line), RRPAR results for the $4d_{3/2}$ subshell; —·—·— (dash-dotted line), RRPA results for the $4d_{5/2}$ subshell; —··— (dash-double-dotted line), RRPA results for the $4d_{3/2}$ subshell.

Because of the overlaps the RRPAR method represents the cross section for a given configuration of the neutral atom. However, the RRPA method appears to give a representation of the total cross section rather than the cross section for leaving the neutral atom in the ground state [4].

One of the authors (V.R.) wishes to acknowledge the hospitality extended by the Department of Physics at the University of Virginia, where part of the present work was completed, and also Turkish Petrol for donation of an IBM RS/5000 computer work station to Marmara University, on which part of the calculations for the present work was performed. This work was partially supported by the U.S. National Science Foundation.

[1] G. Wendin, Phys. Lett. **46A**, 119 (1973); in *Vacuum Ultraviolet Radiation Physics,* edited by E. E. Koch, R. Haensel, and C. Kunz (Vieweg-Pergamon, Braunschweig, 1974), p. 225; Phys. Lett. **51A**, 291 (1975); in *New Trends in Atomic Physics,* edited by G. Grynberg and R. Stora, *Proceedings of the Les Houches Summer School of Theoretical Physics 1982* (North-Holland, Amsterdam, 1984), p. 555.

[2] M. Ya. Amusia, K. Ivanov, and L. V. Chernysheva, Phys. Lett. **59A**, 191 (1976).

[3] H. P. Kelly, S. L. Carter, and B. E. Norum, Phys. Rev. A **25**, 2052 (1982).

[4] V. Radojević, M. Kutzner, and H. P. Kelly, Phys. Rev. A

40, 727 (1989).
[5] W. R. Johnson and C. D. Lin, Phys. Rev. A **20**, 964 (1979); W. R. Johnson, C. D. Lin, K. T. Cheng, and C. M. Lee, Phys. Scr. **21**, 409 (1980).
[6] M. Kutzner, V. Radojević, and H. P. Kelly, Phys. Rev. A **40**, 5052 (1989).
[7] V. Radojević, H. P. Kelly, and W. R. Johnson, Phys. Rev. A **35**, 2117 (1987).
[8] R. D. Mead, A. E. Stevens, and W. C. Lineberger, in *Gas Phase Ion Chemistry,* edited by M. T. Bowers (Academic, New York, 1984), Vol. 3, Chap. 22, pp. 213–248; see also, A. A. Radzig and B. M. Smirnov, *Reference Data on Atoms, Molecules, and Ions* (Springer-Verlag, Berlin, 1985); B. M. Smirnov, *Negative Ions* (McGraw-Hill, New York, 1982).
[9] C. E. Moore, *Atomic Energy Levels,* Natl. Bur. Stand. (U.S.) Circ. No. 35 (U.S. GPO, Washington, D.C., 1971), Vols. I–III.
[10] A. Mandl and H. A. Hyman, Phys. Rev. Lett. **31**, 417 (1973).
[11] M. Neiger, Z. Naturforsch. **A30**, 474 (1975).
[12] J. W. Cooper, Phys. Rev. Lett. **13**, 762 (1964).